Chapter 14
Handling Peak Moments

This chapter is devoted to the subject of local peaks in moment distributions. These occur on top of columns and at receding walls, and for more than one reason structural engineers do not know how to handle them. It is not clear how seriously such peaks must be taken, and how they can be smoothed. An additional problem is the dependency on the mesh fineness; the finer the mesh, the higher the peak. So, the engineer may think to be punished for being serious. This chapter intends to provide practical hints on choosing mesh fineness and designing reinforcement.

14.1 Peaks at Columns

We state the problem for the structure in Figure 14.1. A rectangular concrete slab of length 20 m, width 10 m and thickness 0.6 m with free edges is supported by four inner columns as shown in the figure. The plate is subjected to a homogeneously distributed load $p = 10$ kN/m^2. The material properties are $E = 3 \times 10^7$ kN/m^2 and $\upsilon = 0.2$. A set of axes x, y is chosen with x in the direction of the long edge and y in the short direction. In this section the column is introduced as point support in one single node of the mesh, acting as a ball. We start with square elements of size 0.5 m, which is about slab thickness. This mesh is shown in Figure 14.1.

Figure 14.2 is an assemblage of contour plots and 3D representations for this slab problem. We call the two left-hand columns the left support, and the two right-hand columns the right one. The plots for the displacement w and

J. Blaauwendraad, *Plates and FEM: Surprises and Pitfalls*, Solid Mechanics and Its Applications 171, DOI 10.1007/978-90-481-3596-7_14,

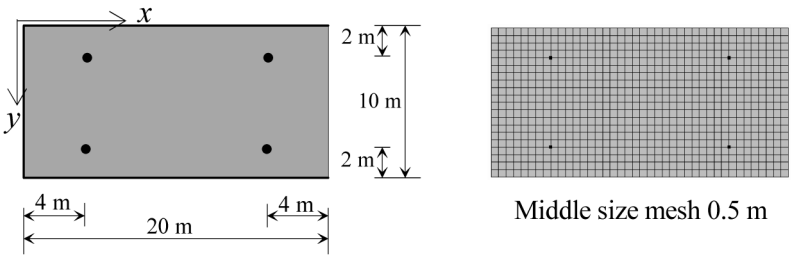

Figure 14.1 Rectangular slab on inward columns.

the bending moment m_{xx} show an almost cylindrical bending between the two supports. In the line over the supports the moment m_{xx} concentrates on top of the columns, which in another way is noted in Figure 14.3. A similar concentration holds for the bending moment m_{yy}. The plot for the twisting moment m_{xy} in Figure 14.2 supports the statement that the horizontal line and vertical line at the supports are more or less lines of symmetry. There the twisting moments are zero. In the four quadrants around the column we notice cloverleaf-type distributions.

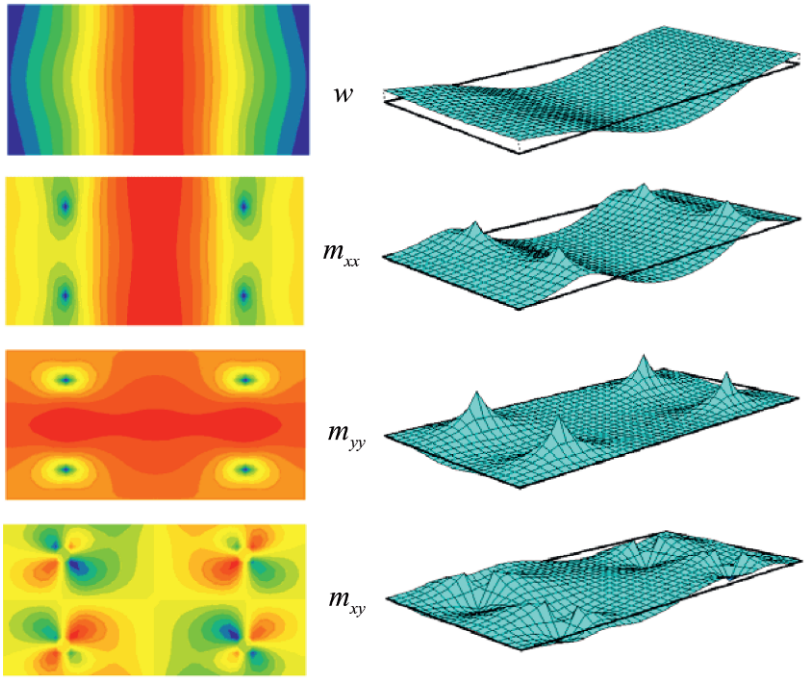

Figure 14.2 Rectangular slab. Both contour plots and 3D presentation.

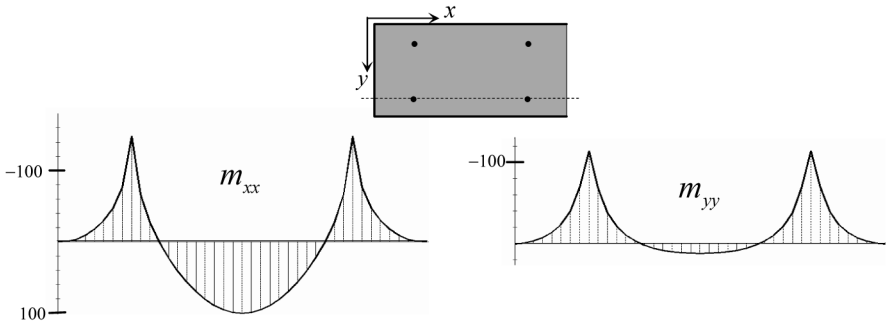

Figure 14.3 Moment diagrams in section over columns.

Next we examine the influence of the mesh fineness, using a commercially available FE code. Figure 14.4 shows the distribution of the moment m_{xx} in the section above the two right columns for three different meshes. Starting from the mesh size 0.5 m we doubled the mesh size to 1.0 m, and then halved it to 0.25 m. When we call the peak moment of the coarsest mesh 100%, then the peak in the medium coarse mesh is 128%, and in the finest 153%. This is not very helpful to the structural designer. But we have other information. We know the exact value of the integral of the moment m_{xx} over the section of the plate; it can be determined from the free body equilibrium of the plate part right of the section under consideration and the p-load on it. We can compare this exact moment with the value which we obtain when we integrate m_{xx} from the FE analysis over the section. If we call the exact moment 100%, then the finest mesh FE mesh delivers 99.2%, the middle 98.9% and the coarsest 97.6%. The largest error in the integrals is about 2%. While the difference in peak between the coarsest and finest mesh is 53%, the integral differs less than 2%! Another observation is that the large difference in value rapidly disappears in the neighbourhood of the column. The moment in the field between two columns is within 1% for all three mesh finenesses.

Lesson on moment peaks

We must not look at the peak value, but at the area of the moment diagram over the section. For this area, it is sufficient to consider a part of the section which extends left and right of the column.

To offer a helping hand, a plate length two times the column width at each side of the column will do, in total five times the column width as in Fig-

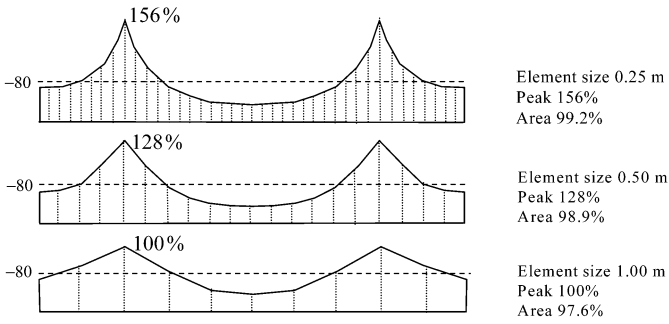

Figure 14.4 Moment distribution for different mesh fineness. The peak values differ much, the areas do not.

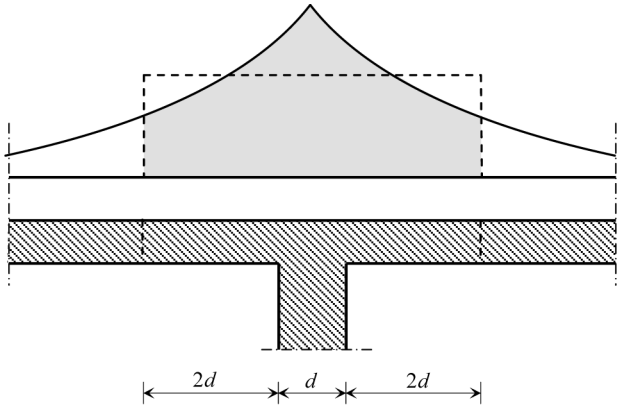

Figure 14.5 Smearing out of moment peak.

ure 14.5. The integral over this section part determines the reinforcement which is needed in this section part. The structural engineer may spread this total amount equally over the width of the section part or choose to spread part of it and concentrate the remaining part above the column. Whatever is chosen, the total amount is the same and is sound.

14.2 Column Reaction Distribution

The previous section has made clear that precise knowledge of the peak moment is not essential for dimensioning the reinforcement. Yet it may support our understanding if we know more about what is happening at a column. For

that purpose we performed an exploratory analysis of the stress problem in the connection between the column and the plate. We simplified the problem to a two-dimensional stress state and performed a membrane-type of analysis. It is understood that the real stress state is axisymmetric, but precise accuracy is not considered necessary. The computed structure is depicted in the left top part of Figure 14.6. It consists of the parts of a horizontal beam and vertical column, cast in one course to a monolithic structure. The left and right edges of this beam are points of counter-flexion with zero moment. There is a downward shear force, which is the load of the structure under consideration. A parabolic load distribution over the thickness is supposed. In the horizontal section between column and beam the vertical stresses are plotted and the position of the resultant for each column half is determined. It appears that this resultant is at a distance two-third of the half column width from the centre line, as depicted in the top right part of the figure. Figure 14.7 shows the distribution over depth of the bending stress at different positions in the beam. Halfway the beam end and the column we see a linear distribution of bending stresses as in beam theory. In the cross-section above the column face the stress distribution has become nonlinear, particularly in the compression zone. In the column centre line the distribution has

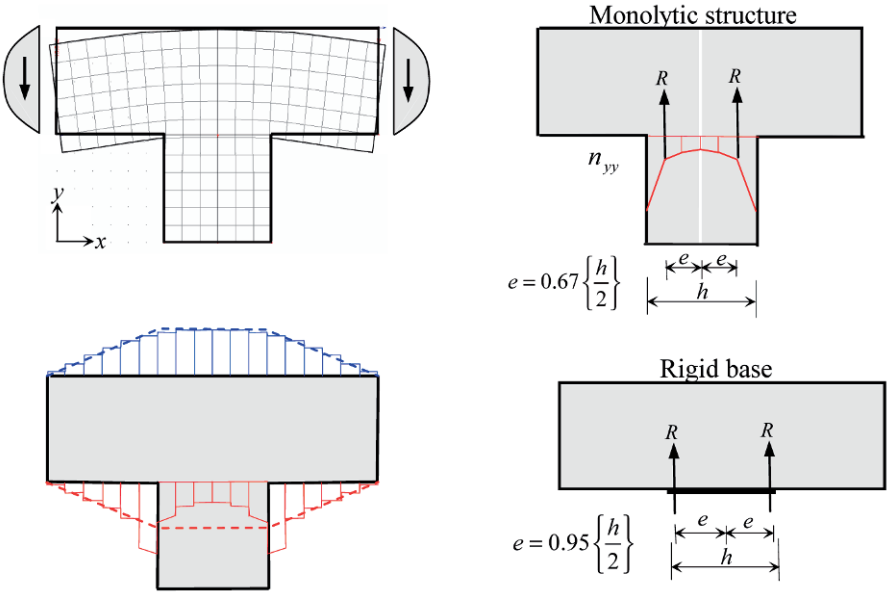

Figure 14.6 Resultant of column reactions.

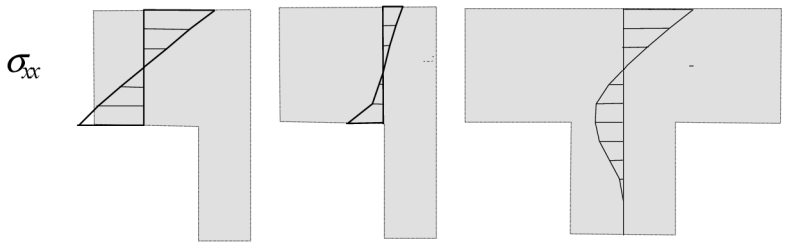

Figure 14.7 Bending stresses in monolytic structure.

even changed further, because now part of the column is taking part in the distribution.

The bottom left part of Figure 14.6 shows the distribution of the bending stresses in the top and bottom faces of the beam. The dashed line presents the stress which would apply according to classical beam theory when just centre-lines are used. Outside the column this classic theory applies practically over the full length. Above the column it does not; there it is disturbed.

Until now in this section we supposed the support of the plate was flexible. We change it into a rigid one in which only compression stresses can be transferred. Such a calculation needs some iteration. The position of the support reactions is shown in the bottom right part of Figure 14.6. The resultant of the vertical stresses over one half column width acts along a line which almost coincides with the face of the column. The distance to the centre line is 95% of the half column width.

The real column situations will lie in the bandwidth which we have covered with the two different cases. The first one is flexible and able to transfer both tensile and compression stresses, and the other is rigid and transfers compression stresses only. The resultant is at a distance to the column face in the order of 10% of the half width ($\frac{1}{2}d$) of the column. We expect that this distance would have been even smaller if we had carried out an axisymmetric analysis. Then the outer material of the column behaves more stiffly because more material is present further from the central axis. We conclude that the reaction is definitely not homogeneously distributed. Instead, it is justified to accept the rule that the reaction acts at the face of the column.

14.3 Application

The message of Section 14.2 will be applied to the structure of Figure 14.1. There the column was introduced as a point support acting on a single node of the mesh. Now we suppose that the column has an area of 0.4×0.4 m^2. This time we have taken an element size of 0.2 m in the analysis. The mesh is unnecessarily small, much smaller than the plate thickness, but this facilitates fitting the column in the mesh. Over the area of the column cross-section there are four elements and nine nodes, of which one coincides with the column centre.

From symmetry considerations we know that the column reaction is 500 kN. We perform three analyses. The first is a repetition of the analysis of Section 14.1, in which the support reaction of 500 kN is introduced as an upward point load in the centre node above the column. In the second analysis we apply the support reaction as a homogeneously distributed load over the column area. In the third analysis the support reaction is introduced as a line load over the perimeter of the column. In all three cases the vertical displacement of the node in the centre of the column is constrained in order to prevent rigid body motions. After completion of the FE analysis the support reaction will be zero, because we have introduced the support reaction as an upward load.

The results of the three analyses for the bending moment m_{xx} in the section over two columns are assembled in Figure 14.8. The maximum moments are -205, -150 and -125 kN respectively. Expressed in terms of the size of the support reaction $R = 500$ kN the results are in absolute values $R/2.3$, $R/3.3$ and $R/4.0$ respectively. The moment in the first analysis (point reaction) is more than 60% higher than in the third (edge load). The value $R/4.0$ for the edge load is in good agreement with the bandwidth expectation of $R/6$ to $R/4$, at which we arrived in Section 7.7 on the basis of the same supposition.

14.4 Cast-Connected Column

Usually columns are fixed to the slab so that moments can be transferred from column to slab. Modelling the column as a one-dimensional line element and fixing it to the slab in one single node will in general evoke high moment peaks in the slab. The same occurs if the column is replaced by a rotational spring in one single slab node. In these cases the conclusions of

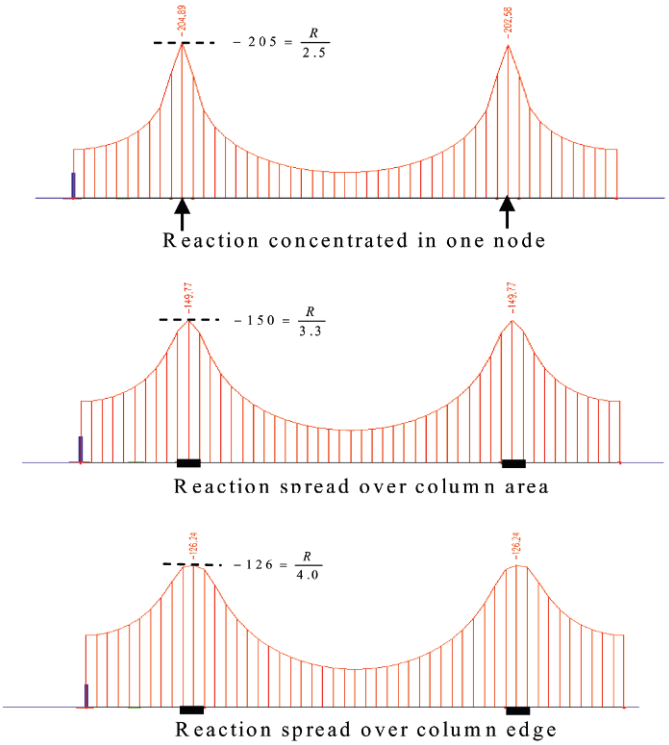

Figure 14.8 Moments in section for different column distribution assumptions.

the preceding section still apply. It is not the peak that is important, but the area of the moment diagram over a section.

There is an alternative way to look at this problem. Structural engineers wonder how to introduce the column in the analysis so that the structural response is closer to the real stress state at the top of the column. One approach is to use distributed springs instead of a lumped rotational spring, either homogeneously distributed over the column cross-section area or as a line distribution along the edge of the area. On the basis of the exploration in Section 14.2 we prefer the edge distribution.

Consider the rectangular cross-section of Figure 14.9 and suppose that this column fits in a mesh of elements. The dimensions of the column cross-section are h and b respectively, where $b < h$. We assume that elements are used with corner nodes only. A lumped spring of constant K is placed in each node. The units of the spring constant are kN/m. Structural engineers tend to choose the value of K such that the axial stiffness EA/l of the column is

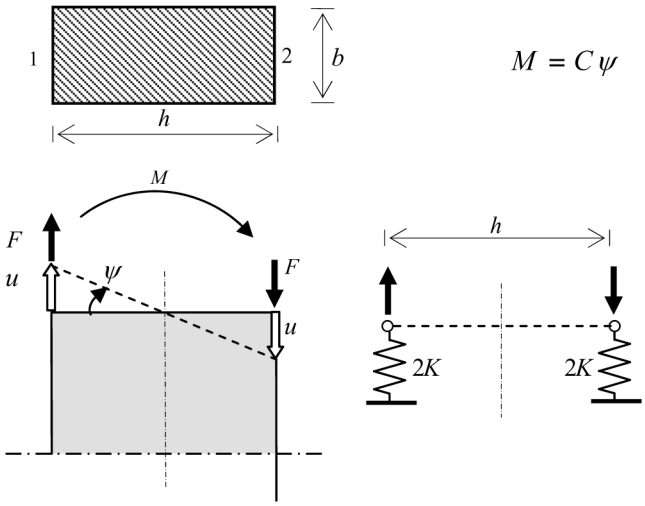

Figure 14.9 Springs on column edge for rotational stiffness.

spread over the four lumped springs, therefore $4K = EA/l$. We will examine how realistic this choice is with respect to the rotational stiffness.

We consider bending of the column about the short axis and apply a moment M, which causes a rotation ψ. We determine the stiffness relation $M = C\psi$, in which C is the rotational spring constant. At a rotation ψ, the two left nodes displace over a distant u, and the right nodes over the same distant in the opposite direction. The force F in two nodes is $F = 2Ku$, and the relation between the displacement and the rotation is $u = \frac{1}{2}h\psi$. Therefore we obtain $F = Kh\psi$. Because of the relation $M = hF$ we find $M = Kh^2\psi$. Therefore, the rotational spring constant is

$$C = Kh^2 \tag{14.1}$$

From the definition of K at the start of the derivation we know

$$K = \frac{1}{4}\frac{EA}{l} \tag{14.2}$$

Substituting this equation in Equation (14.1), and remembering that $I = bh^3/12$, we obtain

$$C = 3\frac{EI}{l} \tag{14.3}$$

This result will appeal to structural engineers: it is the rotational stiffness of a column which is pin-connected at the base, see Figure 14.10. If a column

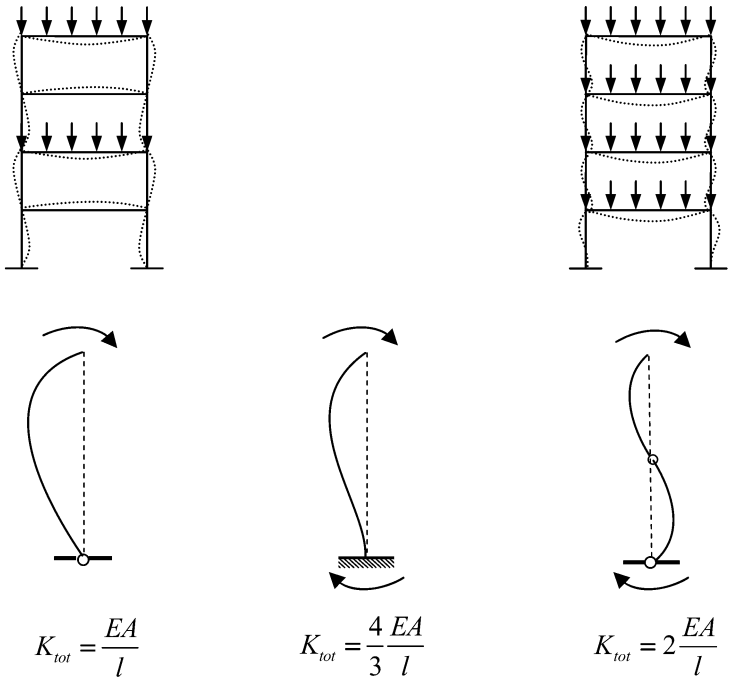

Figure 14.10 Spring constant for different column conditions.

must be simulated which is clamped at the base, the stiffness K must be multiplied by 4/3. If the point of counter-flexion is to act halfway up the column, we must choose a factor 2.

Once more it is stressed that this way of modelling columns requires a mesh, at least around the column, which may be finer than the plate thickness. This approach possibly satisfies the structural engineer, because the maximum moment has some physical meaning. But even in this approach it is wise to determine the integral of the moment distribution in a section in order to know what total reinforcement is required. The improved knowledge about the peak moment then suggests how the reinforcement should be spread over the section.

14.5 Dependence on Program

In the current section we discuss two items together. We meet another type of moment peak, and we address the influence of the choice of program. Fig-

ure 14.1 shows the structure. There is a reinforced concrete floor slab of an apartment building with a balcony. The thickness of the floor is 200 mm and of the balcony 120 mm. The material properties are $E = 3 \times 10^7$ kN/m^2 and $\nu = 0.2$. The floor is subjected to 1.0 kN/m^2 and the balcony to 0.8 kN/m^2. Two providers, I and II, of commercial software have been invited to submit a solution for the bending moments in this plate. We specified that the boundary line coinciding with the y-axis must be considered as clamped and the other wall supports as simply-supported. All three balcony edges are free.

14.5.1 Review of FEM Results

Results of provider I are depicted in Figure 14.11. We will comment on these results first and after that make a comparison with results of provider II. The moment diagram for m_{xx} is drawn for the section at mid-span of and parallel to the simply-supported edges. A negative moment m_{xx} = –8.35 kN occurs at the clamped edge, the moment changes to a positive sign in the middle of the floor, is negative again at the boundary between floor and balcony, and ends with a zero value at the free balcony edge. Along the same section also moment m_{yy} is shown. At the clamped edge it is also negative and has the value -1.66 kN. This value is very close to the product of Poisson's ratio $\nu = 0.2$ and the moment $m_{xx} = -8.35$ kN. This confirms the statement in

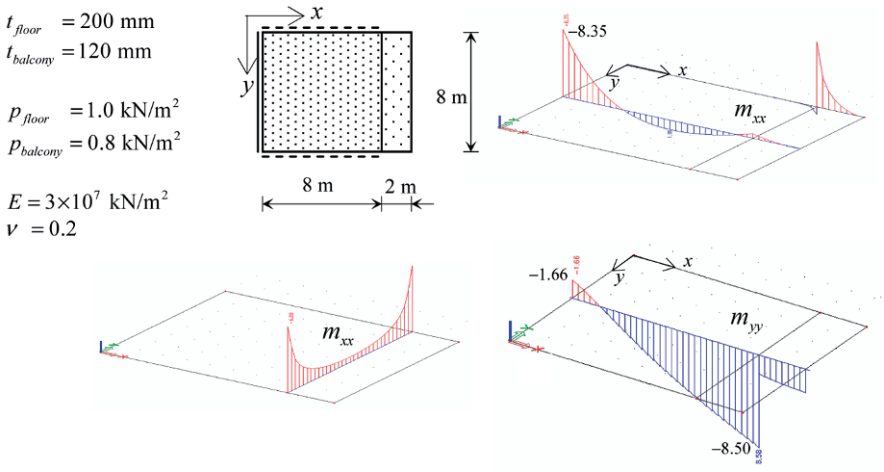

Figure 14.11 Apartment floor with balcony.

Section 4.4.1 that at a clamped edge $m_{yy} = \nu m_{xx}$, where m_{xx} is the moment normal to the edge and m_{yy} in the direction of the edge.

At the boundary between floor and balcony the bending moment m_{xx} is continuous, but the moment m_{yy} appears not to be. According to theory, this must be due to the different flexural rigidities of floor (D_{fl}) and balcony (D_{ba}). It is easily explained for zero Poisson's ratio, but holds generally. Let us write $m_{xx,fl}$ and $m_{xx,ba}$ for floor and balcony respectively. In the same way we write $m_{yy,fl}$ and $m_{yy,ba}$. At the boundary between floor and balcony we have

$$\begin{aligned} m_{xx,fl} &= D_{fl}\,\kappa_{xx,fl} \\ m_{xx,ba} &= D_{ba}\,\kappa_{xx,ba} \end{aligned} \tag{14.4}$$

$$\begin{aligned} m_{yy,fl} &= D_{fl}\,\kappa_{yy,fl} \\ m_{yy,ba} &= D_{ba}\,\kappa_{yy,ba} \end{aligned} \tag{14.5}$$

At the boundary continuity of the moments m_{xx} is required for reasons of equilibrium, and continuity of the curvatures κ_{yy} for reasons of compatibility. Therefore

$$m_{xx,fl} = m_{xx,ba}, \qquad \kappa_{yy,fl} = \kappa_{yy,ba} \tag{14.6}$$

Equality of $m_{xx,fl}$ and $m_{xx,ba}$ delivers, according to Eq. (14.4, different values of $\kappa_{xx,fl}$ and $\kappa_{xx,ba}$, because of the difference between D_{fl} and D_{ba}. This does not play a further role in our consideration. If $\kappa_{yy,fl}$ and $\kappa_{yy,ba}$ are equal, then Eq. (14.5) yields different values of $m_{yy,fl}$ and $m_{yy,ba}$. This explains the discontinuity in m_{yy} in the diagram of Figure 14.11.

14.5.2 Program Comparison

In the discussion of the results of provider I in Section 14.5.1 we did not show a graph for the distribution of moment m_{xx} along the boundary line between floor and balcony. This is the subject of the present section.

We show the diagram for m_{xx} at the boundary between floor and balcony in Figure 14.12 for both provider I and provider II. High concentrations are found at both line ends near the supporting walls. If we consider the free body equilibrium of the balcony we can compute the total moment due to the balcony load which must be transferred in the boundary. Apparently this moment is not evenly distributed along the line, but heavily concentrated at the ends. If we compare the results of the two companies we notice different

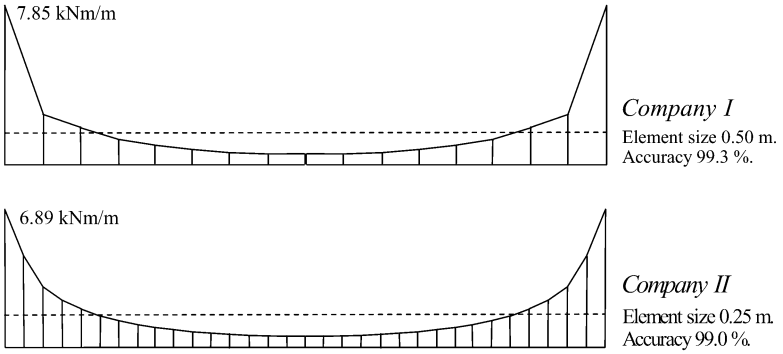

Figure 14.12 Comparison of two FE codes.

peak values, 7.85 and 6.89 kN respectively. The difference is 14%. However, the message, learned for columns, holds here as well. If we integrate the diagram over the length, we obtain moment sums of 99.3 and 99.0% of the exact value, respectively. Again, it is not the peak value that provides the best information, but the area of the moment diagram. Again, the moments at some distance of the peak are virtually the same in both cases. So it is sufficient to determine the diagram area over a short distance at the end of the line. This area needs to be examined for detailing reinforcement in the x-direction at the ends of the boundary line.

Graph output in sections

It is important that FE codes offer the output option for graphs about sections or part of sections.

We now draw attention to the peculiar fact that provider I with the highest peak used the coarsest mesh. In this FE analysis the element size is 0.5 m, while provider II with the lower peak chose a smaller size 0.25 m. This underlines the statement in Section 10.2 that unexpected results may be obtained. It is possible that a higher-order element in combination with a coarse mesh performs better than a fine mesh in combination with a lower-order element.

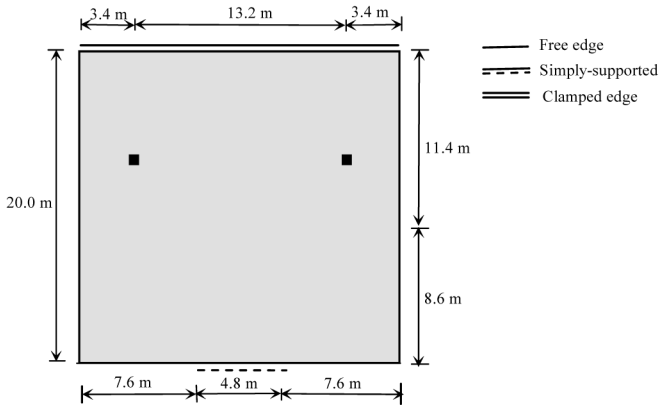

Figure 14.13 Slab for study about user dependency.

14.6 Dependence on User

In this section we show the influence of users on results. This is carried out on a structure with a receding wall. It is another example with a moment peak. The considered floor slab is drawn in Figure 14.13. It has two free edges, one clamped edge (double lines), one edge partly free and partly simply-supported, and two inward placed columns. In this example the rotational stiffness of the columns is specified. The area of the reinforced concrete slab is 20×20 m^2 and the thickness 400 mm. The columns have a cross-section 400×400 mm^2. The design load is 18 kN/m^2, which includes self-weight and variable load, each with accompanying load factors.

We invited structural engineers who attended a continuing education course to design the reinforcement of this slab. At the start we specified a number of of items:

- The concrete cover is 35 mm.
- The mass of hair pins and cutting losses is neglected.
- Concrete properties are $E = 3 \times 10^7$ kN/m^2, $\upsilon = 0.2$.
- Steel yield stress is 435 N/mm^2.
- If possible, Kirchhoff theory is used.
- Ignore crack widths and deflections; only ULS is considered.
- Codes of practice requirements for minimum reinforcement are disregarded.
- The lever arm in the cross-section is 0.9 times the effective plate thickness.

The structural engineers were asked to submit

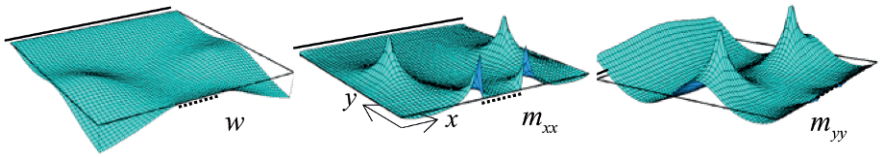

Figure 14.14 Deflection and moments for slab of Figure 14.13.

- The peak values of the moments at the column support.
- The total mass of reinforcement in kilograms.
- A subdivision of the total amount of reinforcement needed for the four meshes, two in the top layers and two in the bottom layers.

The invitation to structural engineers was repeated for five subsequent courses in place-country-region Belgium and The Netherlands. We show the result of one of these five courses, which is representative for all. Eighteen people in the course participated, and they used six different commercial FE codes. Two of them just provided moment values and did not submit an amount of reinforcement. We will first show some FE results. They come from an analysis with small elements such that the column support matches with 2×2 elements. Figure 14.14 shows a 3D plot of the deflection and bending moments m_{xx} and m_{yy}. Figure 14.15 shows the distribution of m_{xx} and m_{yy} over two important sections. The values of m_{xy} are small and therefore omitted. The peak values of the bending moment in Figure 14.15 are in the bandwidth 400 to 450 kNm/m: the peak moment is approximately $M =$ 425 kNm/m. The column support reaction R is 1880 kN. The ratio of R to

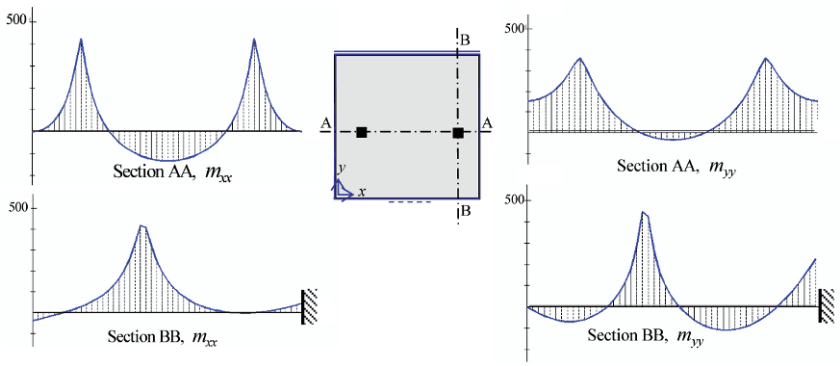

Figure 14.15 Moment diagrams in sections.

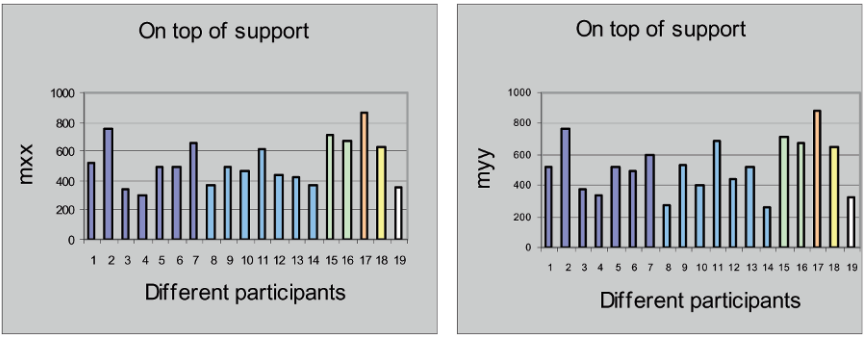

Figure 14.16 Moments at column by different participants.

m is 4.5, close to the expected ratio 5 which we expect in a grid of columns, as discussed in Section 7.7 and depicted in Figure 7.13.

We now will discuss the submissions of the participants. Figure 14.16 is a bar chart for the moments m_{xx} and m_{yy} at the column support. The 18 participants obtained moment peaks differing by more than a factor of two. Bars with the same colour have been obtained with the same FE code.

Lesson

Using the same program does not necessarily lead to similar results; the user can make a difference.

In Section 14.1 we explained that the difference in peak value should not be a big problem in the design of reinforcement; we work with areas of the moment diagram rather than with peak values. Then no large differences in reinforcement amount are to be expected. However, reality is different. In Figure 14.17 both the total amount is shown and the subdivision over the two orthogonal reinforcement layers in both top and bottom of the slab. The differences between the participants are substantial.

As stated, the experiment has been repeated several times with other groups of experienced structural designers, always with a similar outcome. Do engineers think ‘iron is cheaper than brains’? Many engineers place reinforcement where it is not necessary for strength reasons.

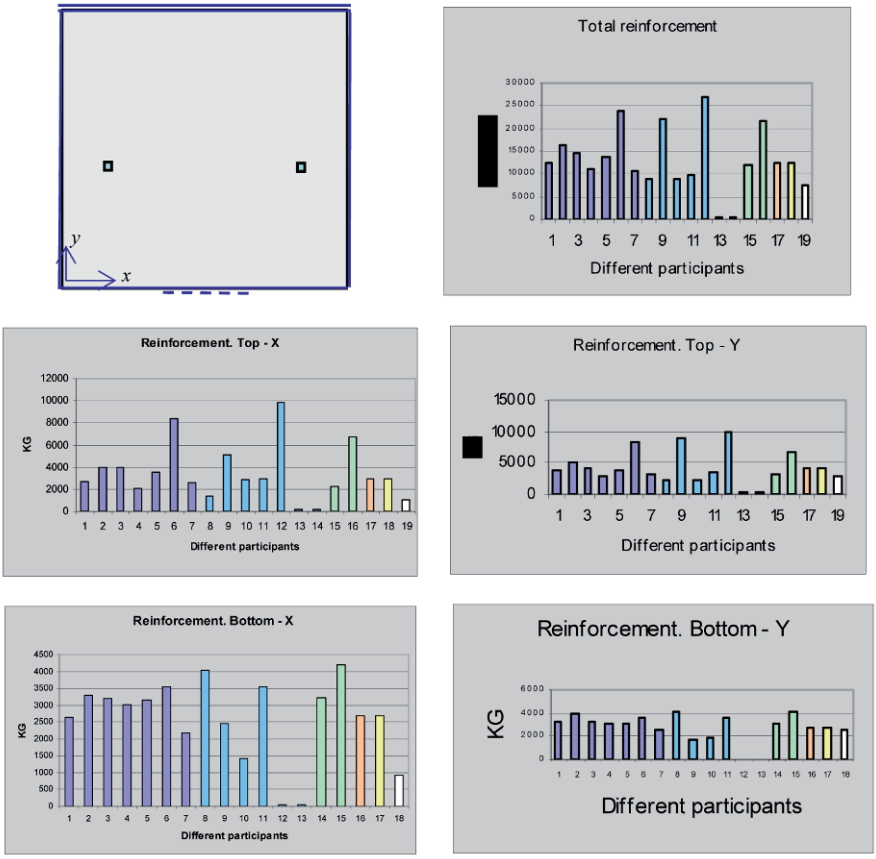

Figure 14.17 Reinforcement demand by different participants.

Lesson

Different structural engineers come to very different amounts of reinforcement for the same structure and load.

14.7 Impact of Support Flexibility and Concrete Cracking

In Sections 14.1 and 14.5.2 we considered the moment integral over a section in the plate and compared it to the exact moment due to the load.

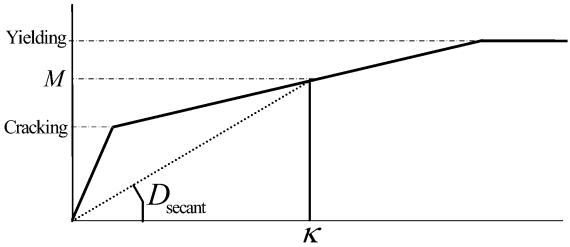

Figure 14.18 Moment-curvature diagram of reinforced concrete cross-section.

There we were able to calculate the total moment due to the load in the considered section from simple equilibrium considerations. This is not always possible. In the top left part of Figure 14.18 we show a structure supported by both a wall and two columns, such that the wall end and the columns are not in one line. We consider the FE result for m_{yy} (direction parallel to the wall) in the section over the end of the wall. Again we want to compare the area of this moment diagram to the exact value of the total moment. For that purpose we must consider the free body equilibrium of a plate part including the columns. We must now account for the support reactions; these are a result of the FE analysis and, as stated in Chapter 10, very reliable. They are in perfect equilibrium with the loads. So, we are able to calculate the total moment due to load and support reactions and can perform a check on the area of the computed m_{xx}-diagram. We omit the calculations and just report that again we obtained a very good match.

We proceed with the example to show the impact of introducing flexibility of the wall support and accounting for cracking. For that reason we again consider the distribution of the moment m_{yy} in the section over the end of the wall and perform three calculations. In the first calculation all nodes in the line where the wall occurs are rigid supports. There the displacement w is zero. In the second analysis we replace the rigid supports by flexible ones by inserting springs in the z-direction. The spring constant is EA/l where E is Young's modulus of the wall concrete, A is the cross-section of the wall part which is assigned to a node, and l the height of one storey. In the third analysis we return to the rigid supports and reduce the plate rigidity D in order to account for cracking. Due to cracking, the rigidity easily halves at large moments compared to D for uncracked concrete. Figure 14.18 illustrates this statement. Large negative moments occur on the tops of the wall and columns. Therefore we introduce a reduction of 50% for the two rows of elements left and right of the wall and the four elements around

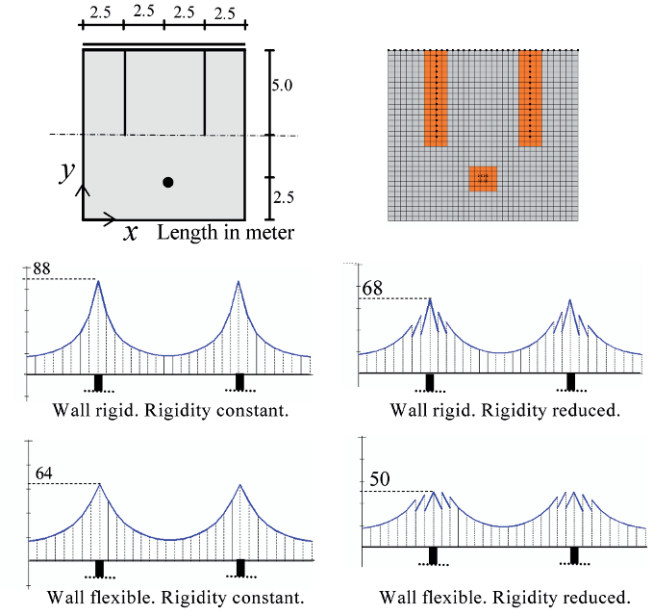

Figure 14.19 Study about impact of flexible wall and reduced rigidity.

the columns. In the fourth analysis we finally combine wall spring supports with reduced plate rigidity.

Figure 14.19 shows the results for the four analyses. We notice considerable differences in the peak values of the moment m_{xx}. For rigid wall supports and uncracked plate rigidity the maximum moment value is 88 kN. Inserting only wall flexibility makes the value reduce to 64 kN, a reduction of 28%. Reducing only the plate rigidity results in 68 kN, a reduction of 23%. The combination of springs and cracking leads to a moment 50 kN. Now the reduction has increased to 43%. We conclude that adapting plate rigidity decreases moments in the order of 20%, and the combination of rigidity decrease and wall flexibility in the order of 40%.

Use of flexible supports

This small investigation teaches us that it is worthwhile to introduce realistic conditions. The correct value of the spring constant is not a critical issue. Introducing flexibility makes the difference. After that,

halving or doubling the spring constant no longer has much effect. Similarly it is worth accounting for cracking by reducing the plate rigidity.

The moment reduces significantly, and (not shown in this example) deflections will increase substantially. Of course, the choice made here is subjective and has just the intention to show the effect. It makes clear that realistic moment-curvature diagrams must be consulted for fixing rigidities when FE codes make predictions about deflections in the serviceability state.

Commercially available FE codes are starting to offer checking facilities on deflections. The programs must be able to handle orthotropic plate properties as discussed in Section 3.5. In this orthotropic case m_{xy} and m_{yx} are equal so $m_{av} = m_{xy}$. Also D_{xy} and D_{yx}, defined in Eq. (3.46), are equal so $D_{\text{av}} = D_{xy}$. Therefore we must know the rigidities in the constitutive equations

$$\begin{Bmatrix} m_{xx} \\ m_{yy} \\ m_{xy} \end{Bmatrix} = \begin{bmatrix} D_{xx} & D_\nu & 0 \\ D_\nu & D_{yy} & 0 \\ 0 & 0 & D_{xy} \end{bmatrix} \begin{Bmatrix} \kappa_{xx} \\ \kappa_{yy} \\ \rho_{xy} \end{Bmatrix} \tag{14.7}$$

A first analysis is done with constant plate rigidity D to determine the moments and design the reinforcement. Then the moment-curvature diagrams for x- and y-direction are calculated for each element. From the first analysis we know the bending moments m_{xx} and m_{yy}, and from the moment-curvature diagrams we derive the curvatures κ_{xx} and κ_{yy}. From this new rigidities D_{xx} and D_{yy} are found. It is not clear which off-diagonal rigidity D_ν must be used. A practical value is

$$D_\nu = \nu\sqrt{D_{xx} D_{yy}} \tag{14.8}$$

which leads to the correct term in the isotropic case. The value of Poisson's ratio ν can be made dependent on the size of the moments. For an uncracked cross-section the value 0.2 is fine, and as the reinforcement starts to yield the value should be set to zero. Between the cracking moment and yield moment a linear interpolation might be chosen.

It remains to choose a value for the torsion rigidity D_{xy} which holds for the value m_{xy} from the first analysis. With reference to Section 11.6.2 and Chapter 16 we may assume that this twisting moment raises reinforcement forces which are conforming with bending moments $m_{xx} = m_{xy}$ and $m_{yy} =$

m_{xy}. At these bending moment values we read rigidities D_{xx} and D_{yy} from the moment-curvature diagrams. Then we may apply the formula

$$D_{xy} = \frac{1}{2}(1-\nu)\sqrt{D_{xx}D_{yy}} \tag{14.9}$$

A physical ground for this approach does not exist other than the statement that the correct rigidity is obtained for the limiting case of isotropy.

The second linear-elastic FE analysis with adapted rigidities will yield moment values different from the first analysis. Therefore the procedure of rigidity adaptation must be repeated and a further analysis is necessary. This is done until the results do not change anymore in a practical sense. Therefore, the final moment values and deflections are the result of an iterative procedure.

After completing the iteration procedure we can also compute crack widths. From the moments we know the steel strains in the reinforcement bars and can pronounce an expectation on the crack widths, following the codes of practice rules.

14.7.1 Application of Finite Element Program

We show an application with the commercial FE code *Diamonds* (Buildsoft, Belgium). This program chose its cracking formula from the Eurocode 2 (EN 1992-1-1). The curvature α in the cracked state is calculated by the formula

$$\alpha = \zeta\alpha_{\parallel} + (1-\zeta)\alpha_{|} \tag{14.10}$$

where $\alpha_{|}$ is the curvature for the uncracked section and $\alpha_{\parallel}$ the curvature for the fully cracked section (the section consisting of concrete compression zone and reinforcement). The distribution coefficient ζ is

$$\zeta = 1 - \beta(\sigma_{\mathrm{sr}}/\sigma_s)^2 \tag{14.11}$$

Here β is a coefficient accounting for the influence of the duration of the loading or of repeated loading on the average strain (1.0 for single short-term loading; 0.5 for sustained loads or many cycles of repeated loading); σ_s is the stress in the reinforcement calculated on the basis of a cracked section; σ_{sr} is that same stress but under the loading conditions causing first cracking. The curvature α is used to derive the reduced rigidity in the element stiffness matrix.

According to Eurocode 2 (EN 1992-1-1) the crack width is

$$w_k = s_{r,\max}(\varepsilon_{sm} - \varepsilon_{cm}) \tag{14.12}$$

where $s_{r,\max}$ is the maximum crack spacing in the principal stress direction. It is calculated from

$$\frac{1}{s_{r,\max}} = \frac{\cos\theta}{s_{r,\max,x}} + \frac{\sin\theta}{s_{r,\max,y}} \tag{14.13}$$

Here θ is the angle between the axes of the principal stress and the direction of the reinforcement, and $s_{r,\max,x}$ and $s_{r,\max,y}$ are the crack widths in the reinforcement directions; they are defined by

$$s_{r,\max} = k_3\, c + k_1 k_2 k_4\, \phi/\rho_{p,\text{eff}} \tag{14.14}$$

where

k_3 = 3.4
C = cover of longitudinal reinforcement
k_1 = 0,8 (high bond bars)
k_2 = $(\varepsilon_1 + \varepsilon_2)/2\,\varepsilon_1$
ε_1 and ε_2 are (tensile) strains at the boundaries of the cracked section;
ε_1 is the greater stress
k_4 = 0.425
ϕ = bar diameter
$\rho_{p,\text{eff}}$ = $A_s/A_{c,\text{eff}}$

The factor $\varepsilon_{sm} - \varepsilon_{cm}$ in Equation (14.12) is the difference between the mean strain in the reinforcement and the mean strain in the concrete between cracks under the relevant combination of loads

$$\varepsilon_{sm} - \varepsilon_{cm} = \frac{\sigma_s - k_t \frac{f_{ct,\text{eff}}}{\rho_{p,\text{eff}}}\left(1 + \alpha_e \rho_{p,\text{eff}}\right)}{E_s} \geq 0.6\frac{\sigma_s}{E_s} \tag{14.15}$$

where

σ_s = stress in the tension reinforcement assuming a cracked section
α_e = ratio E_s/E_{cm}
k_t = 0.4 for long term loading
$f_{ct,\text{eff}}$ = tensile strength of the concrete

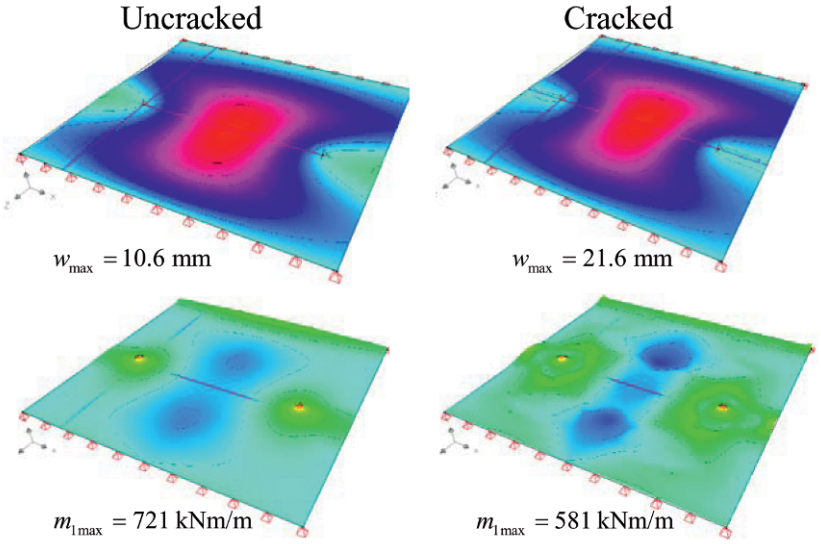

Figure 14.20 Results of FE code for deflections and moments.

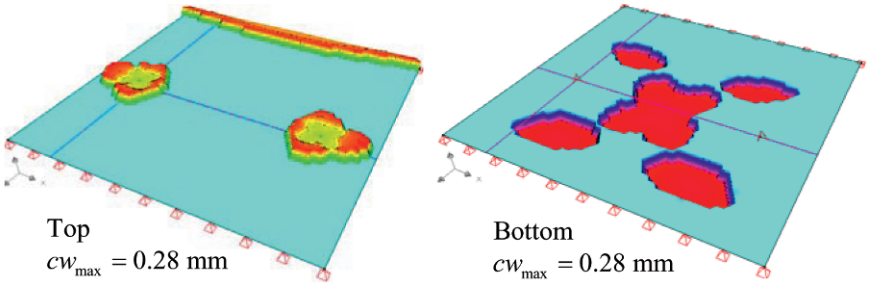

Figure 14.21 Results of FE code for crack widths.

Normally the bar diameter ϕ is not known in the design process. In this case a fictive diameter is used defined as $\sqrt{(2A_s/3\pi)}$; (six bars lead to A_s).

Figure 14.20 shows results of an analysis for a rectangular slab, supported at two parallel edges and two inner columns, both for ULS and SLS. The ultimate limit state was considered for the moments (safety), and the serviceability limit state for the deflections (normal practice). The left three plots in the figure are for the un-cracked slab; the right plots are for the cracked slab. Note that the deflection increases from 10.6 to 21.6 mm due to cracking. The maximum value of the principal moment m_1 for ULS decreases from 721 to 581 kNm/m; this is the order of 20%, mentioned earlier. Notice that the peak

moment localizes in the uncracked state, and smears out in the cracked state. Figure 14.21 shows crack widths for SLS in the upper and lower face.

14.8 Message of the Chapter

- We need to focus on the area of the bending moment diagram and not on the peak bending moments. That area, representing the total moment to be transferred by the section, is in equilibrium with the load and support reactions.
- It is possible to pass a judgement on the real peak value. The column reaction can be best distributed over the perimeter of the cross-section of the column. The value of the bending moment is, in conformance with Chapter 7, in the bandwidth of one-sixth to one-fourth of the column reaction force.
- Cast-connected columns, capable of loading the slab by a lumped moment, can be modelled by springs on the edge of the column cross-section.
- FE analysis results are dependent on the chosen FE code and on the user. Different programs for the same problem lead to different solutions. Higher-order elements may produce a lower peak than lower-order elements with a finer mesh.
- Design of reinforcement depends strongly on the individual structural engineer.
- The introduction of springs at hard support spots and accounting for severe cracking at moment peaks makes moments spread out over larger widths and reduces maximum values.
- FE codes should offer the output option of section graphs for deflections, moments and shear forces. It should also be possible to specify a special part of a section. The FE code should output integrals over the (part of the) section.